Lab on a Chip



View Article Online PAPER



Single-step assembly of asymmetric vesicles

Cite this: Lab Chip, 2019, 19, 749

Laura R. Arriaga, ¹⁰†‡^a Yuting Huang, †a Shin-Hyun Kim, ¹⁰b Juan L. Aragones, ¹⁰c

Asymmetric vesicles are membranes in which amphiphiles are asymmetrically distributed between each membrane leaflet. This asymmetry dictates chemical and physical properties of these vesicles, enabling their use as more realistic models of biological cell membranes, which also are asymmetric, and improves their potential for drug delivery and cosmetic applications. However, their fabrication is difficult as the selfassembly of amphiphiles always leads to symmetric vesicles. Here, we report the use of water-in-oil-in-oilin-water triple emulsion drops to direct the assembly of the two leaflets to form asymmetric vesicles. Different compositions of amphiphiles are dissolved in each of the two oil shells of the triple emulsion; the amphiphiles diffuse to the interfaces and adsorb differentially at each of the two oil/water interfaces of the triple emulsion. These middle oil phases dewet from the innermost water cores of the triple emulsion drops, leading to the formation of membranes with degrees of asymmetry up to 70%. The triple emulsion drops are fabricated using capillary microfluidics, enabling production of highly monodisperse drops at rates as high as 300 Hz. Vesicles produced by this method can very efficiently encapsulate many different ingredients; this further enhances the utility of asymmetric vesicles as artificial cells, bioreactors and delivery vehicles

Received 23rd August 2018, Accepted 15th January 2019

DOI: 10.1039/c8lc00882e

rsc.li/loc

Introduction

Asymmetric vesicles are unsupported membranes made of amphiphilic lipids or polymers, in which the composition of the inner leaflet of the membrane is different from that of the outer. It is the presence of these compositional asymmetries that makes the chemical and physical properties of biological cell membranes so rich.1 Thus, the use of vesicles as models for studies of the properties of cells should preferably use asymmetric vesicles.² Similarly, such asymmetric membranes may also increase the utility of vesicles for drug delivery and cosmetic applications. For example, the toughness of a polymer could be combined with the biocompatibility and functionality of a lipid, resulting in a hybrid delivery vehicle with improved mechanical stability. Moreover, expensive and precious lipids intended to interact with certain surface receptors could be located selectively only in the outer membrane monolayer, while unspecific and cheaper

lipids can be used in the inner monolayer. Unfortunately,

conventional methods for the production of vesicles rely on the random self-assembly of amphiphilic molecules in an aqueous environment, and only vield vesicles with symmetric membranes.4 There are some strategies for producing asymmetric membranes. For example, molecules that sequester amphiphiles from the membrane, such as cyclodextrins,⁵ or molecules that facilitate their flip flop, such as flipases, ⁶ yield vesicles with partial asymmetry. Moreover, vesicles can be formed from planar membranes using an inkjet printer;⁷ if these planar membranes are asymmetric, membranes that are asymmetric will be produced.8 However, these methods have very low throughputs that limit their use for applications. Alternatively, vesicles can be formed using emulsion drops as templates, enabling preparation of vesicles with asymmetric membranes through the assembly of one membrane leaflet on the surface of the drop and the independent assembly of the second membrane leaflet, consisting of a different lipid, on a planar interface through which the drop is passed to form the bilayer.3 While the throughput is better using this method, many of the drops are still destroyed upon passing through the interface and they have large heterogeneity in size and composition. Implementation of the emulsion method in multi-step, PDMS based microfluidic devices significantly improves its performance.9 For example, starting with water-in-oil (W/O) emulsions stabilized by a first type of phospholipids and captured in a static droplets array in a PDMS device, asymmetric vesicles can be formed as a new oil

^a School of Engineering and Applied Science and Department of Physics, Harvard University, 02138 Cambridge, MA, USA. E-mail: weitz@seas.harvard.edu

^b Department of Chemical and Biomolecular Engineering, KAIST, 305-701 Daejeon,

^c Department of Material Science and Engineering, Massachusetts Institute of Technology, 02139 Cambridge, MA, USA

[†] These authors contributed equally to this work.

[‡] Present address: Departamento de Ingenieria Quimica Industrial y del Medio Ambiente, Escuela Tecnica Superior de Ingenieros Industriales, Universidad Politecnica de Madrid, 28006 Madrid, Spain.

phase, containing a second type of phospholipids, passes over the droplets and deposits a different monolayer. 9c However, the production of vesicles using this method does not generate vesicles continuously and thus is not truly high-throughput. Alternatively, PDMS devices based on having two flowfocusing regimes have generated asymmetric vesicles with higher throughput. 9d,e For example, W/O emulsions stabilized by one lipid leaflet can be generated in a first flow-focusing regime, while the second lipid leaflet can be fabricated onto the emulsions in a second flow-focusing regime; this strategy yields asymmetric vesicles from aqueous dispersions of phospholipids.^{9d} However, these aqueous dispersions likely consists of multillamelar vesicles (MLVs) with different sizes and compositions, which must disassemble upon adsorption at the W/O interface to form the first lipid leaflet of the asymmetric vesicle. To adsorb at the W/O interface, MLVs must first diffuse to the interface; the diffusion of smaller MLVs will be faster than that of the bigger ones. Moreover, once adsorbed, MLVs must disassemble to cover the interface; this phenomenon might be dependent on lipid composition. Therefore, both size and composition differences in the MLV dispersion will make it difficult to control lipid composition when using aqueous dispersions of lipid mixtures. Alternatively, asymmetric vesicles can be formed using double emulsion drops as templates. For this, the double emulsion template needs to be assembled in two separate steps, which can be performed within a single PDMS chip. 9e In this approach, W/O emulsions stabilized by one lipid leaflet are first formed, then transferred into a second oil containing a second type of lipids, and finally re-emulsified into W/O/W double emulsion drops. Extraction of the oil from the final double emulsion out of the chip results in asymmetric vesicle formation. 9e Unfortunately, this method requires careful control of multiple flow-focusing regimes simultaneously, making the device challenging to operate; the use of PDMS material also disallows many common lipid solvents and limits the number of potential applications. Therefore, it is crucial to develop an alternative microfluidic strategy in which both leaflets are produced in a single-step in a glass device. Improved methods for producing asymmetric vesicles with microfluidics would

Here, we report a microfluidic approach for the continuous production of monodisperse vesicles with asymmetric membranes using water-in-oil-in-oil-in-water (W/O/O/W) triple emulsion drops, produced in a single-step, as templates, as illustrated schematically in Fig. 1. These triple emulsion drops have two ultra-thin oil shells, both made of the same oil but each one containing a different lipid composition. The lipids initially dissolved in the inner oil phase predominantly adsorb at the inner oil/inner water interface, whereas the lipids initially dissolved in the outer oil phase predominantly adsorb at the outer oil/outer water interface; this results in the formation of W/O/W double emulsion drops with asymmetric interfacial compositions. Dewetting of the middle oil phase from the innermost water cores of these double emulsions induces the formation of the vesicle bilayer, which preserves

make their utility and applicability much greater.

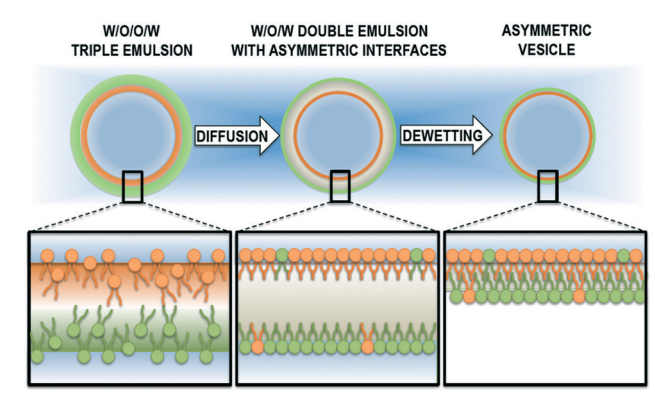


Fig. 1 Schematic illustration of the spontaneous processes involved in the assembly of asymmetric vesicles using water-in-oil-in-oil-in-water triple emulsion drops as templates.

the asymmetric composition of the emulsions that we use as templates. Using this approach we produce lipid vesicles with degrees of asymmetries up to 70%.

Experimental

Chemicals

The lipids, 1,2-dioleoyl-*sn-glycero*-3-phosphocholine (DOPC) and 1,2-dioleoyl-*sn-glycero*-3-phosphoethanolamine-*N*-(biotinyl) (sodium salt) (DOPE-Biotinyl) are purchased from Avanti Polar Lipids Inc. The fluorescent protein streptavidinfluorescein isothiocyanate (ST-FITC) is purchased from Invitrogen. Dextran from *Leuconostoc Spp.* (70 KDa), poly(vinyl alcohol) (PVA, 13–23 kDa, 87–89% hydrolyzed) and sucrose, along with the organic solvents, chloroform and hexane, are all purchased from Sigma. The phosphate buffered saline (PBS) solution is purchased from ThermoFisher Scientific. Milli-Q water from a Millipore system (resistivity 18.2 $\mathrm{M}\Omega~\mathrm{cm}^{-1}$) is used to prepare the aqueous phases. All aqueous phases are filtered through 5 $\mu\mathrm{m}$ filters (Acrodisc) before their injection in the microfluidic device.

Fabrication of the glass capillary device

Square borosilicate glass capillaries with internal diameter 1.05 mm are purchased from Atlantic International Technology. Round, single barrel standard borosilicate glass capillaries with external diameter 1.00 mm and internal diameter 0.58 mm are purchased from World Precision Instruments. Both square and round capillaries are shaped using a micropipette puller (P-97, Sutter Instrument, Inc.). In particular, we make a constriction in the square capillary and taper the round capillaries to a diameter tip of 20 µm. We then use sand paper (2500 grit) to open the diameter tips to 60 and 120 µm, for the injection and collection capillaries respectively. injection capillary is treated trimethoxy(octadecyl) silane, purchased from Sigma, to make it hydrophobic, whereas the collection capillary is treated with 2-[methoxy(polyethyleneoxy)9-12propyl] trimethoxysilane, purchased from Gelest, to render its surface hydrophilic. The tips of these two capillaries are immersed in the silanes for

about 15-30 min and later dried using compressed air. Two additional round capillaries are stretched using a burner to a typical external diameter of about 100-200 µm and used without further treatment. The device is assembled onto a glass microscope slide. First, the square capillary is fixed to the slide with 5 min epoxy (Devcon). Then, the two round tapered and silanized capillaries are inserted in the opposite ends of the square capillaries, the injection capillary on the left and the collection capillary on the right. Their axis are then aligned on a microscope, leaving a separation distance between the two capillaries of about 80 µm, and their positions are fixed to the slide with epoxy. Next, we insert one of the stretched capillaries inside the round injection capillary and the second stretched capillary in the interstices between the square and the round injection capillaries. These are also fixed to the slide using epoxy. Finally, we place dispensing needles with luer lock connection (0.5" needle length, 20 gauge), purchased from McMaster-Carr, at the junctions between capillaries or their ends, and fixed them to the slide with epoxy. We leave the 5 min epoxy to completely cure for 24 hours before injecting any liquids into the device.

Operation of the glass capillary device

We use 5 pumps (PHD 2000 Infusion, Harvard Apparatus), an inverted microscope (Leica, with a 5x dry objective), and a high-speed camera (Phantom V9) to conveniently operate this glass capillary device. The three water phases are kept in 10 mL Becton Plastic syringes, whereas the two oil phases are kept in 5 mL Hamilton Gastight syringes. Each syringe is placed on a pump and connected with polyethylene tubing of inner diameter 0.86 mm (Scientific Commodities, Inc.) to one of the device inlets; this enables us to inject each phase at the adequate flow rate to form water-in-oil-in-oil-in-water triple emulsion drops with thin oil shells.

Asymmetry measurements

The asymmetry of the vesicles is determined from the fluorescence intensity of the membrane relative to the background at the vesicle equatorial plane. To perform these measurements, we acquire confocal fluorescence images of individual vesicles using a 10x dry objective with a numerical aperture of 0.3 on a confocal microscope (Leica) and an argon laser (488 nm) as excitation source for the ST-FITC. We use a custom MATLAB code to measure the fluorescence intensity of the vesicle membrane relative to the background. The code identifies the vesicle membrane as the circumference formed by the pixels with maximum intensity and returns the radial intensity distribution, as exemplified in Fig. 3(B, left).

Brownian dynamics simulations

We consider a three-dimensional system of N = 1372 spheres of mass m and diameter σ to represent the lipid molecules. These particles are suspended in a solvent with temperature T and viscosity η at constant volume V. The number density of particles ρ is 0.0035. The motion of these Brownian parti-

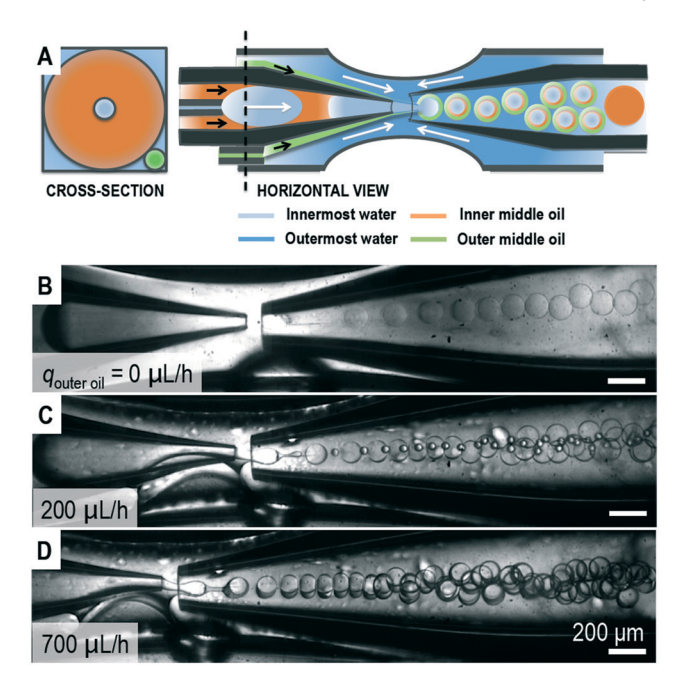


Fig. 2 (A) Schematic illustration of the cross-section and horizontal view of the microfluidic device used to produce water-in-oil-in-oil-inwater triple emulsion drops. The cross-section corresponds to the position of the dashed line in the horizontal view. (B-D) Optical microscope images showing production of (B) double and (C and D) triple emulsion droplets at flow rates, q, of the innermost water, inner middle oil and outermost water phases of 700, 700 and 3000 μL h⁻¹, respectively, and at flow rates of the outer middle oil phase of 0, 200 and 700 μ L h⁻¹, respectively. The smaller capillary for injection of the outer middle oil phase is out of the field of view in images B-D.

obeys cles the overdamped Langevin equation. $\partial_i r_i = \beta F_i + \sqrt{2D} \Lambda_i(t)$, where r_i is the position of particle i at time t, β the inverse thermal energy, and $D = k_B T/3\pi \eta \sigma$ is the diffusion coefficient, being $k_{\rm B}$ the Boltzmann constant. Since in the overdamped regime the inertial term is neglected, we consider the differences in the molecular masses of the lipid molecules M by means of the size of the particles, assuming that lipids are spheres of homogeneous density equal to unity and thus $M = (1/6)\pi\sigma^3$. Therefore, the total conservative force acting on the particle i, Fi, only takes into account excluded volume interactions, modelled with the Weeks-Chandler-Andersen (WCA) potential, which determines the interaction strength, ε , and the time scale, $\tau = \sigma^2/(\varepsilon\beta D)$. $\Lambda_i(t)$ is a stochastic force with zero mean and unit standard deviation, accounting for the collisions with the solvent molecules. We use $D = 0.08\sigma^2/\tau$, and apply periodic boundary conditions along the y and z axis, while the simulation box is bounded along the x axis by two adsorbing interfaces, which are modelled as harmonic potentials of the form $U(x) = (1/2)k(x_0)$ $(-x)^2$, where x_0 is the position of the interface. Particles closer than one particle diameter are tethered to this interface.

Results and discussion

To fabricate W/O/O/W triple emulsion drops, we use a glass capillary microfluidic device that consists of two round

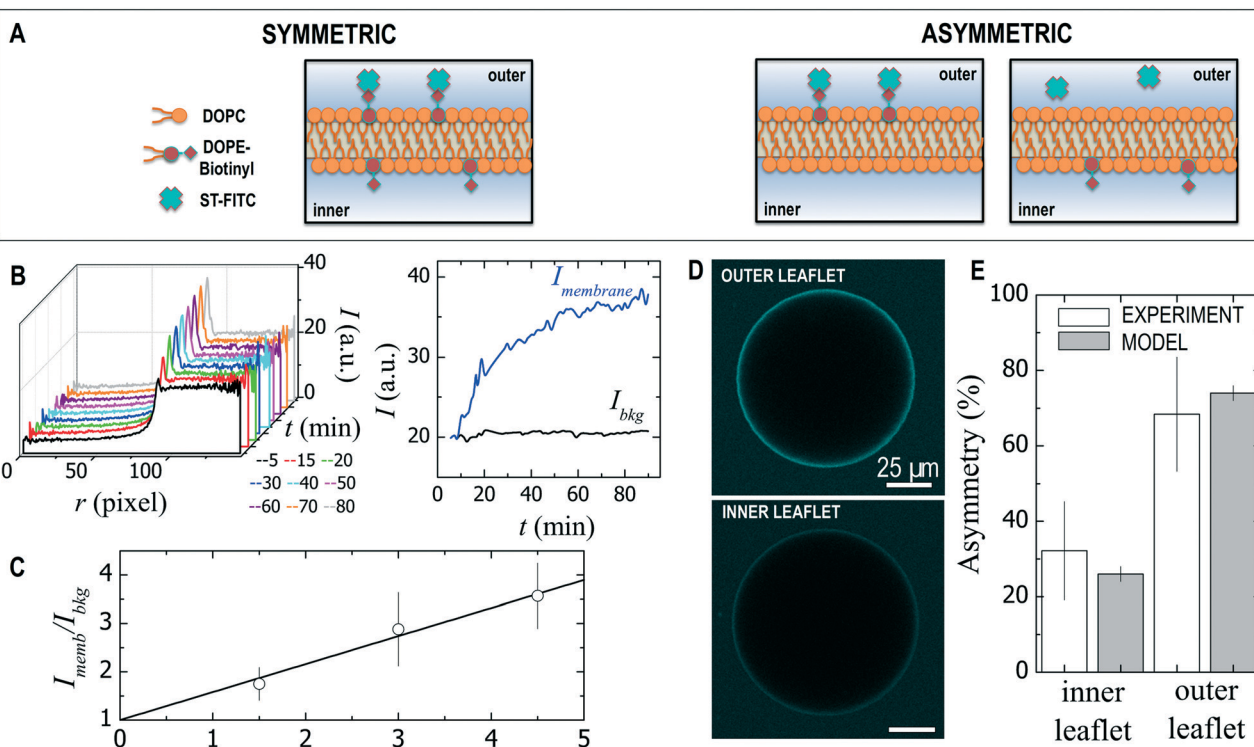


Fig. 3 (A) Schematic illustration of the biotin-streptavidin assay used to measure the degree of asymmetry in asymmetric phospholipid vesicles. (B) Kinetics of the interaction of streptavidin with biotin: Time evolution of (left) radial intensity distribution of vesicles and (right) intensity of the vesicle membrane (blue) and background (black) during diffusion of streptavidin to the outer leaflet of the lipid membrane. These data are measured in a vesicle containing 3 mol% of DOPE-Biotinyl molecules in each lipid leaflet. (C) Variation of the intensity of the membrane relative to the background as a function of the molar fraction of DOPE-Biotinyl molecules in the outer leaflet of the vesicle membrane prepared from triple emulsion drops that initially contain the same quantity of DOPE-Biotinyl molecules in both middle oil layers (symmetric vesicles). (D) Representative confocal fluorescence microscope images showing binding of streptavidin to biotin for asymmetric vesicles prepared from triple emulsion drops that initially contain DOPE-Biotinyl molecules in either the outer (top) or the inner (bottom) middle oil phases. (E) Asymmetry in the distribution of DOPE-Biotinyl molecules of the resultant vesicles. Hollow bars are experimental data and solid bars the theoretical prediction from diffusion (simulation data).

capillaries inserted into the opposite ends of a square capillary. The outer dimension of these round capillaries fits the inner dimension of the square capillary; this configuration aligns the axes of these two round capillaries. Two additional smaller round capillaries are inserted on the left side of the square capillary for injection of additional fluids. One of these is inserted into the main injection capillary and the other one into one of the interstices between the main injection capillary and the square capillary, as illustrated schematically by the cross-section of the device shown in Fig. 2(A). In addition, to help focus the flow of the four fluids required to form these triple emulsion drops, we incorporate a constriction in the square capillary, as illustrated schematically by the horizontal view of the device shown in Fig. 2(A). The innermost water phase is injected into the smaller capillary that is located inside the main injection capillary; this water phase consists of an aqueous solution that contains 9 wt% dextran (70 kDa), 1 wt% polyvinyl alcohol (PVA, 13-23 kDa) and 250 mM sucrose, where dextran is chosen to provide the adequate viscosity for microfluidic production, PVA is chosen

 $c_{\mathrm{Biotin}} \, (\mathrm{mol\%})$

to enhance the stability of triple emulsion drops, and sucrose is used to help balance the osmolarity with the collection solution. The inner middle phase is a 5 mg mL⁻¹ lipid solution dissolved in a mixture of 36 vol% chloroform and 64 vol% hexane and is injected into the main injection capillary. We treat this main injection capillary with trimethoxy (octadecyl) silane to render its walls hydrophobic. This enables the inner water phase to form a train of plug-like water drops that do not contact the internal capillary wall; instead, these are surrounded by the inner middle oil phase, which forms a very thin layer at the internal wall of the main injection capillary. The outer middle oil phase is injected into the second smaller capillary, which is located in the interstices between the main injection capillary and the square capillary. Inserting this single smaller capillary in one of the interstices between the round and square capillary is enough to create a three-dimensional flow that completely wets the outer wall of the round capillary. This second oil phase also consists of a 5 mg mL⁻¹ lipid solution dissolved in a mixture of 36 vol% chloroform and 64 vol% hexane; however, the lipid

composition is different than that of the inner middle oil phase, and this ultimately creates an asymmetry between the compositions of the inner and outer membrane leaflets. When the middle oil phase exits this second smaller capillary, it co-flows with the outermost aqueous phase, while contacting the outer wall of the hydrophobic main injection capillary, as illustrated schematically in Fig. 2(A). An additional aqueous phase is then injected into the interstices between the main round and square capillaries on the right to better flow-focus all the phases. Both outermost water phases consist of 10 wt% PVA aqueous solutions. This configuration enables breakup of the plug-like water droplets and oil phases into triple emulsion drops. These triple emulsion drops flow into the collection capillary. To avoid wetting of the triple emulsions on the internal walls of the collection capillary, we coat it with pegylated silane; this renders its walls hydrophilic. To avoid any osmotic stress that may induce rupture of triple emulsions, we collect them into a large volumetric excess of phosphate buffered saline (PBS) solution that matches the osmolarity of the innermost water phase.

To use double or triple emulsion drops as templates to form symmetric or asymmetric vesicles, respectively, it is important to control the thickness of the oil shell of these emulsions as this limits the spontaneous removal of the oil from their shells.10 Our microfluidic device enables control of the shell thickness of the triple emulsion drops by varying the flow rate of the outer middle oil phase. For example, if we fix the flow rate, q, of the innermost water and inner middle oil phases to 700 µL h⁻¹ each, and the flow rate of the two outermost water phases to 3000 µL h⁻¹ each, we fabricate double emulsion drops with ultrathin shells, as shown in Fig. 2(B); these have shell thicknesses below 1 μ m. The shell thickness is determined from the volume of the single O/W drop that results from double emulsion rupture, which is calculated from the diameter measured in optical microscope images. 11 Injection of the outer oil phase at a flow rate of 200 $\mu L\ h^{-1}$ or lower results in the formation of triple emulsion drops with thin shells, as shown in Fig. 2(C). In this case, the oil shell of the triple emulsion remains thin due to the formation of satellite oil droplets between triple emulsions; these are easily separated upon collection from the triple emulsions based on their difference in density. Increasing the flow rate of the outer oil phase to 700 μ L h⁻¹ results in the formation of triple emulsion drops with thicker shells as shown in Fig. 2(D). The shell thickness of these emulsions can be increased further upon increasing the flow rate of the outer middle oil phase.

These triple emulsion droplets spontaneously yield vesicles if both the mixture of solvents of the two middle phases and the shell thickness of the template are carefully chosen. ^{10,12} The solvents of the two middle phases consist of a mixture of chloroform and hexane at a volume ratio close to but still below the cloud point of the lipid mixture that ultimately forms the vesicle membrane. Chloroform is a good solvent for lipids and thus enables them to remain fully dissolved during fabrication of the templates. However, it is highly volatile and starts to evaporate as soon as the emulsion drops exit the de-

vice and enter the collection vial. Inside this collection vial, the chloroform continues to diffuse out from the shell to the water, thereby making the shell rich in hexane, which is a poor solvent for the lipids. Therefore, as lipids continue to adsorb at the two O/W interfaces of the triple emulsion drops, they start to precipitate due to the reduction in the solvent quality; this induces an attraction between the two monolayers of lipids and the ultimate formation of a bilayer membrane. 10,13 However, the range of this attraction strongly depends on the size of the amphiphile and thus the shell thickness must be chosen accordingly. For example, vesicles made of low molecular weight amphiphiles, like phospholipids, are spontaneously obtained only using triple emulsion drops with very thin shells, like those shown in Fig. 2(C), whereas vesicles made of larger molecular weight amphiphiles, like polymers, are spontaneously obtained even using emulsions with thicker shells, ¹⁴ as those shown in Fig. 2(D).

The vesicles produced using this approach are not perfectly unilamellar. Similarly to symmetric vesicles produced from double emulsion templates, 10 our vesicles frequently contain a patch made of aggregated excess lipid in a certain region of the lipid bilayer. The concentration of lipid in the oil phase is optimized to form a single bilayer; however, small differences in triple emulsion drop size or oil shell thickness results in having a larger or smaller number of lipid molecules than that required for optimal packing of lipids in a bilayer membrane. While having a larger number of lipid molecules results in lipid patch formation, having a smaller number results in breakage of triple emulsions upon solvent dewetting.

To measure the degree of asymmetry, which we define as the differences in composition between the two membrane leaflets, we fabricate vesicles from triple emulsion drops that contain a 100 mol% of 1,2-dioleoyl-sn-glycero-3-phosphocoline (DOPC) in one of the thin oil layers and a mixture consisting of 94 mol% DOPC and 6 mol% 1,2-dioleoyl-sn-glycero-3phosphoethanolamine-N-(biotinyl) (sodium salt) (DOPE-Biotinyl) in the other, as illustrated schematically in Fig. 3(A). As a calibration, we also prepare symmetric vesicles from triple emulsion drops with identical compositions in both membrane leaflets, containing 1.5, 3 and 4.5 mol% of DOPE-Biotinyl in each oil layer. After vesicle formation, which involves thinning of the oil shell of the emulsion templates due to chloroform diffusion to the aqueous phase and observation of hexane dewetting, we add 0.05 mg mL⁻¹ of fluorescently labelled streptavidin (ST-FITC) to the outer phase of the vesicle suspension. During incubation of the vesicles with ST-FITC, we measure the fluorescence intensity of the membrane relative to the background at the equatorial plane of the vesicles using a confocal fluorescence microscope. We observe that the intensity of the membrane achieves a plateau value approximately 90 minutes after incubation, as shown in the rightmost panel of Fig. 3(B). We therefore incubate the vesicles with ST-FITC for 90 min in all the experiments. Our calibration shows that the membrane intensity increases proportionally to the concentration of DOPE-Biotinyl in the outer

leaflet of the membrane as shown in Fig. 3(C). We use this calibration to determine the concentration of DOPE-Biotinyl located at the outer membrane leaflet from confocal images of asymmetric vesicles, as exemplified in Fig. 3(D). We obtain an asymmetry of about 70% in the distribution of DOPE-Biotinyl molecules, as shown by the white bars in Fig. 3(E). Flip-flop or intra-bilayer translocation of phospholipids is hampered by a significant energy barrier and thus occurs over time periods as long as approximately 100 h, ¹⁵ which is the typical shelf life of the vesicles that we produce. There-

fore, this type of motion is out of our experimental window.

Moreover, once the vesicles are formed, there is no longer an

oil shell as in the emulsion templates; instead, we have a

lipid bilayer or membrane that cannot experience further

thinning. Accordingly, we observe that the degree of asymme-

try measured is maintained for at least 24 h.

Other methods to measure asymmetry include fluorescence correlation spectroscopy measurements on fluorescently labelled phospholipids, ¹⁶ and selective quenching of fluorescently labelled phospholipids located in the outer membrane leaflet.³ Alternatively, we choose the biotinstreptavidin assay described above, because in addition to the determination of the degree of asymmetry, this assay demonstrates the potential of our functionalized asymmetric vesicles for protein binding in the outer membrane leaflet. Indeed, this experiment demonstrates the formation of asymmetric vesicles with optically uniform streptavidin coronas.

We hypothesize that the diffusion of the phospholipids towards the O/W interfaces of the triple emulsions determines the degree of asymmetry obtained with this thin shell approach. To test this hypothesis, we simulate the diffusion of the phospholipids used in the experiments as the diffusion of spherical particles confined between two flat interfaces. In our simulations, 6% of the total number of particles is slightly larger than the other 94% to represent DOPE-Biotinyl molecules, shown by the blue spheres in Fig. 4(A); these are initially confined in half of the total width of the simulation box to model one of the oil layers of the triple emulsion drops. The rest of the particles, shown by the red spheres in Fig. 4(A), extend through the whole width of the simulation box. Using this model, we observe that the number of DOPE-Biotinyl molecules that adsorb to the O/W interface to which they are initially closer represents about 70% of the total number of DOPE-Biotinyl molecules when adsorption of particles at the interface is completed, as shown by the blue line in Fig. 4(B). About 30% of the total number of DOPE-Biotinyl molecules is thus found at the O/W interface to which they are initially further when adsorption is completed, as shown by the red line in Fig. 4(B). This result is in good agreement with the asymmetry that we experimentally measure, as shown in Fig. 3(E), and therefore this model can be used to predict the degree of asymmetry achievable by our experimental approach. Using this model, we first explore the effect of increasing the percentage of blue spheres on the degree of asymmetry of the vesicles produced from triple emulsion drops with two oil shells of identical thickness, as summa-

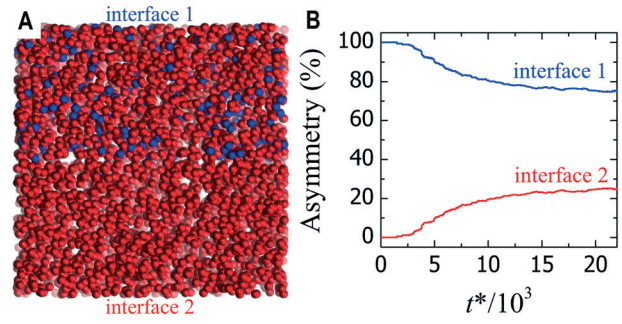


Fig. 4 (A) Illustration of the initial configuration used to model diffusion of lipids within the oil shells of the triple emulsion droplets. One of the oil layers, which occupies half of the width of the simulation box contains 6% of blue and 94% of red particles, whereas the other half contains 100% of red particles. Blue particles mimic DOPE-Biotinyl molecules, whereas red particles mimic DOPC molecules. (B) Variation of the number of blue particles over the total number of blue particles at the two interfaces of the simulation box as a function of time t^* in reduced units. $t^* = t/r$.

rized in Table 1. We find that the asymmetry remains of about 78% upon increasing the percentage of blue spheres up to 9% when blue and red spheres have the same reduced mass. We also observe that the asymmetry remains of about 74% if the ratio of masses between blue and red particles is varied to 1.25, which represents the ratio of molecular weight between the DOPE-Biotinyl and the DOPC molecules used in the experiments. To reflect more biologically relevant systems, we also explore the degree of asymmetry predicted by our model for the asymmetric distribution of a prototype ganglioside, monosialotetrahexosylganglioside (GM1), in a DOPC-based membrane. To do this, we next consider the ratio of masses between red and blue particles to be 2.1; this again results in a degree of asymmetry of approximately 75%.

We then explore the effect of increasing the thickness of the oil layer that is initially free of blue particles on the asymmetry of the vesicles. Importantly, our simulation model shows that the asymmetry of the vesicle membrane can be increased controlling the relative thicknesses of each layer as summarized in Table 2. Indeed, an asymmetry of about 90% can be potentially achieved upon making the thickness of the oil layer that is initially free of DOPE-Biotinyl molecules 5 times larger

Table 1 Percentage of blue particles at the interface to which they are initially closer (asymmetry) for different initial percentages of blue particles and an initial configuration to model diffusion similar to that sketched in Fig. 4(A)

	$m_{\rm b}=m_{\rm r}^{\ a}$	$m_{\mathrm{b}}=1.25m_{\mathrm{r}}$	$m_{\rm b}=2.1m_{\rm r}$
$\frac{N_{\rm b}/(N_{\rm b}+N_{\rm r})^b\ (\%)}{N_{\rm b}/(N_{\rm b}+N_{\rm r})^b\ (\%)}$	$N_{\mathrm{b,i}}/N_{\mathrm{b}}^{c}$ (%)	$N_{\rm b,i}/N_{\rm b}$ (%)	$N_{\rm b,i}/N_{\rm b}$ (%)
3	75(3)	76(3)	78(5)
6	76(2)	74(2)	75(4)
9	78(2)	77(3)	77(4)

 $[^]a$ $m_{\rm b}$ and $m_{\rm r}$ are the mass of blue and red particles, respectively. b $N_{\rm b}$ and $N_{\rm r}$ are the total number of blue and red particles, respectively. c $N_{\rm b,i}$ is the number of blue particles at the interface to which they are initially closer. Standard deviations are in parentheses.

Table 2 Percentage of blue particles at the interface to which they are initially closer (asymmetry) for 6% of blue particles initially confined within the oil layer of smaller thickness

$h_{\rm i}/h_{ m o}^{\ a}$	$N_{\mathrm{b,i}}/N_{\mathrm{b}}^{\;b}$ (%)
1/2	76(2)
1/3	86(3)
1/4	88(4)
1/5	89(4)
1/6	92(4)

 a h_{i} and h_{o} are the thickness of the inner middle and outer middle oil phases of the triple emulsion drops, respectively. b N_b is the total number of blue particles and $N_{\rm b,i}$ is the number of blue particles at the interface to which they are initially closer. Standard deviations are in parentheses.

than that of the second oil layer. Our model, however, does not take into account the slow shell thinning that occurs upon chloroform diffusion to the aqueous phases or the sudden dewetting of the hexane-rich solvent from the emulsions; unfortunately, these could limit the experimental degree of asymmetry achievable by our approach to the reported 70% value, even in the case of a larger second oil shell.

The high-throughput microfluidic approach here described, in which both leaflets are produced in a single step using triple emulsion drops as templates, produces degrees of asymmetry lower than those reported for high-throughput microfluidic implementations of the phase transfer method, in a single chip, as summarized in Table 3. The stability of the degree of asymmetry is comparable to those reported, as expected from the large energy barrier that hampers lipid translocation. However, our device has the unique advantage of being made of glass. Therefore, its applicability is not restricted by the use of certain oils; vesicle design can involve any type of solvent and thus any type of lipids, making this

Table 3 Summary of the capabilities of the main methods reported to date to produce asymmetric vesicles, including the steps involved (procedure), procedure type, degree of asymmetry achieved, time stability of the asymmetry and a summary of the advantages and disadvantages of the different methods. The approach here reported appears in the last row

Method	Procedure	Туре	Asymmetry	Asymmetry stability	Advantages	Disadvantages	Ref.
Cyclodextrin (CD)	1) Electroformation 2) CD addition	Bulk	Partial	≥4 h	Solvent-free Ease of implementation	Polydisperse sizes and compositions Low encapsulation Low throughput	5 <i>c</i>
Inverse emulsion phase transfer	1) W/O drops formation 2) Centrifugation through O/W interface	Bulk	80-95%	≥24 h	Ease of implementation	Polydisperse sizes Low encapsulation Low throughput	3
	1) W/O drops formation 2) Centrifugation through O/W interface	1) Micofluidic 2) Bulk	85%	<15 h	Monodisperse sizes High encapsulation	Tedious bulk step Low throughput	9 <i>a</i>
	1) W/O drops formation 2) Transference to water	Microfluidic (single chip)			Monodisperse sizes High encapsulation High throughput	Polydisperse Compositions Limited number of solvents (PDMS)	9 <i>d</i>
Layer-by-layer	W/O drops formation Transference to oil Transference to water	Microfluidic (single chip)	100%		Experiments in production chip Monodisperse sizes and compositions High encapsulation	Vesicles remain in chip Low throughput Limited number of solvents (PDMS)	9 <i>c</i>
Inkjet printing	Formation of SUVs Injection in W/O drops to form a lipid bilayer Inkjet printing	1) Bulk 2) Chip 3) Inkjet printing		≥1 h	Monodisperse sizes High encapsulation	Low throughput	8
Double emulsion	1) W/O drops formation 2) W/O/W double emulsion drop formation 3) Solvent removal	Microfluidic (single chip)	90-95%	≥30 h	Monodisperse sizes and compositions High encapsulation High throughput	Limited number of solvents (PDMS)	9 <i>e</i>
Triple emulsion	1) W/O/O/W triple emulsion drop formation 2) Solvent removal	Microfluidic (single chip)	70%	≥24 h	Monodisperse sizes and compositions High encapsulation High throughput Single-step Versatility of solvents (glass)	Residual oil pocket or excess lipid aggregate	

technique much more versatile than currently available PDMSbased approaches. Below their melting transition temperature, the solubility in oil of long chain fatty acids and triacylglycerols decreases upon increasing their melting point;¹⁷ this likely points to the difficulty of dissolving solid lipids in PDMScompatible solvents as mineral oil or 1-octanol. Prominent examples of solid lipids are ceramides, gangliosides and other lipopolysaccharides rich in saturated chains. In addition, it has been shown than the extraction of gangliosides, which can be extracted using a chloroform/methanol mixture, is inefficient if the mixture is substituted by hexane/isopropanol. 18 Moreover, dissolution in oil of charged lipids like the negatively charged phosphoethanolamine (PE) or phosphoglycerol (PG) is likely difficult due to the charged hydrophobic moiety if they additionaly have large saturated chains. In all these cases a chip made in glass will be significantly advantageous.

Conclusions

We report a single-step microfluidic approach based on the use of W/O/O/W triple emulsion templates that enables the high-throughput production of vesicles with asymmetric membranes. Moreover, these vesicles have uniform sizes and compositions. Using this approach, we fabricate lipid vesicles with degrees of asymmetry of approximately 70%. The degree of asymmetry of the vesicle membrane is limited by the diffusion of the lipids from the oil shells of the templates to the O/W interfaces. Therefore, strategies that control the relative rate of diffusion of each type of molecule to the interfaces may enable the degree of asymmetry of the vesicle membrane to be increased. For example, controlling the relative thicknesses of each layer or inserting an intervening third layer of oil with no lipids should lead to an increased degree of asymmetry. These templates should also be useful to fabricate polymer vesicles and hybrid polymer/lipid vesicles, broadening the range of materials that can be used. Moreover, this fabrication method enables highly efficient encapsulation of ingredients within the membrane since the innermost fluid is injected from a completely different fluid stream than the outermost. Thus, our results should greatly increase the utility of vesicles as model biological membranes or for drug delivery and cosmetic applications through the use of these asymmetric vesicles.

Conflicts of interest

There are no conflicts to declare.

Acknowledgements

This work was supported by the National Science Foundation (DMR-1310266 and DMR-1705775), the Harvard Materials Research Science and Engineering Center (DMR-1420570), and a Marie Curie International Outgoing Fellowship within the EU Seventh Framework Programme for Research and Technological Development (PIOF-2012-332078). We thank W. Lloyd Ung for helpful discussions on device design.

Notes and references

- 1 (a) P. F. Devaux, Biochemistry, 1991, 30, 1163; (b) G. van Meer, D. R. Voelker and G. W. Feigenson, Nat. Rev. Mol. Cell Biol., 2008, 9, 112; B. Fadeel and D. Xue, Crit. Rev. Biochem. Mol. Biol., 2009, 44, 264.
- 2 (a) K. Berndl, J. Kas, R. Lipowsky, E. Sackmann and U. Seifert, Europhys. Lett., 1990, 13, 659; (b) Y. Elani, S. Purushothaman, P. J. Booth, J. M. Seddon, N. J. Brooks, R. V. Law and O. Ces, Chem. Commun., 2015, 51, 6976; (c) L. Lu, W. J. Doak, J. W. Schertzer and P. R. Chiarot, Soft Matter, 2016, 12, 7521-7528.
- 3 S. Pautot, B. J. Frisken and D. A. Weitz, Proc. Natl. Acad. Sci. U. S. A., 2003, 100, 10718.
- 4 (a) F. Szoka and D. Papahadjopoulos, Proc. Natl. Acad. Sci. U. S. A., 1978, 75, 4194; (b) M. I. Angelova and D. S. Dimitrov, Faraday Discuss. Chem. Soc., 1986, 81, 303.
- 5 (a) H. T. Cheng, Megha and E. London, J. Biol. Chem., 2009, 284, 6079; (b) H. T. Cheng and E. London, Biophys. J., 2011, 100, 2671; (c) S. Chiantia, P. Schwille, A. S. Klymchenko and E. London, Biophys. J., 2011, 100, L1.
- 6 J. M. Boon and B. D. Smith, Med. Res. Rev., 2002, 22, 251.
- 7 (a) J. C. Stachowiak, D. L. Richmond, T. H. Li, A. P. Liu, S. H. Parekh and D. A. Fletcher, Proc. Natl. Acad. Sci. U. S. A., 2008, 105, 4697; (b) J. C. Stachowiak, D. L. Richmond, T. H. Li, F. Brochard-Wyart and D. A. Fletcher, Lab Chip, 2009, 9, 2003.
- 8 D. L. Richmond, E. M. Schmid, S. Martens, J. C. Stachowiak, N. Liska and D. A. Fletcher, Proc. Natl. Acad. Sci. U. S. A., 2011, 108, 9431.
- 9 (a) P. C. Hu, S. Li and N. Malmstadt, ACS Appl. Mater. Interfaces, 2011, 3, 1434; (b) K. Nishimura, H. Suzuki, T. Toyota and T. Yomo, J. Colloid Interface Sci., 2012, 376, 119; (c) S. Matosevic and B. M. Paegel, Nat. Chem., 2013, 5, 958; (d) K. Karamdad, R. V. Law, J. M. Seddon, N. J. Brooks and O. Ces, Chem. Commun., 2016, 52, 5277; (e) L. Lu, J. W. Schertzer and P. R. Chiarot, Lab Chip, 2015, 15, 3591.
- L. R. Arriaga, S. S. Datta, S.-H. Kim, E. Amstad, T. E. Kodger, F. Monroy and D. A. Weitz, Small, 2014, 10, 950.
- 11 S.-H. Kim, J. W. Kim, J.-C. Cho and D. A. Weitz, Lab Chip, 2011, 11, 3162.
- 12 T. Foster, K. D. Dorfman and H. T. Davis, J. Colloid Interface Sci., 2010, 351, 140.
- 13 A. R. Thiam, N. Bremond and J. Bibette, Langmuir, 2012, 28, 6291.
- 14 (a) R. C. Hayward, A. S. Utada, N. Dan and D. A. Weitz, Langmuir, 2006, 22, 4457; (b) H. C. Shum, J.-W. Kim and D. A. Weitz, J. Am. Chem. Soc., 2008, 130, 9543; (c) H. C. Shum, E. Santanach-Carreras, J.-W. Kim, A. Ehrlicher, J. Bibette and D. A. Weitz, J. Am. Chem. Soc., 2011, 133, 4420.
- 15 T. G. Pomorski and A. K. Menon, Prog. Lipid Res., 2016, 64,
- 16 S. Chiantia, P. Schwille, A. S. Klymchenko and E. London, Biophys. J., 2011, 100, L1.
- 17 J. S. Patton, B. Stone, C. Papa, R. Abramowitz and S. H. Yalkowsky, J. Lipid Res., 1984, 25, 189.
- 18 A. Hara and N. S. Radin, Anal. Biochem., 1978, 90, 420.